1. Carbon Cycle & Ocean Modelling

An understanding of the carbon cycle and ocean processes and circulation is a very important component in the development of earth system models. At CSIR-4PI we have been actively engaged in several aspects of this study, especially in the determination of fluxes between atmosphere, ocean and land, through modelling and measurements, Modelling of biogeochemical cycles of carbon, nitrogen, phosphorous, trace metals and oxygen in the ocean, WMO-standard measurements of greenhouse gases and analysis and a detailed study of the decadal variability of sea surface temperature (SST) formed the major activities of the group.

With the use of the Modular Ocean Model and a complex biogeochemical model called TOPAZ, we examined the oxygen cycle very closely in the Arabian Sea. The presence of a suboxic zone in the Arabian Sea is well known, but quantification of the contributors to this depletion is still under debate. With the help of our model, we established the roles of primary production in oxygen production and remineralisation and nitrification in it consumption. The extents of the oxygen minimum zones were simulated very well. Hanle in Ladakh is an extremely clean site uncontaminated by local sources. It is ideally suited for the measurement of the background carbon dioxide concentration which could reflect the global increase of carbon in the atmosphere from year to year. WMO-standard carbon dioxide measurements here showed an in increase of 2.5 ppm in the annual average from 2019 to 2020 which translated to an atmospheric loading of 5.3 Gigatonnes of carbon in 2020. Methane increased by 15 ppb in the same period. Measurements at Hoskote, near Bangalore, showed similar increases in carbon dioxide and methane. No significant change in carbon monoxide was noticed while nitrous oxide showed a secular increase.

A new orthogonal decomposition procedure involving annual mean, low and high frequency components was applied to study sea surface temperature anomalies from 1950-2010. There was a pronounced asymmetry between northern and southern hemispheres. Sixteen high variability clusters were identified of which six were in the Arctic indicating the vigorous changes happening there.

Inside:

- Suboxic Zone in the Arabian Sea and Bay of Bengal
- Greenhouse gases data collection and analysis

1.1 Suboxic Zone in the Arabian Sea and Bay of Bengal

Analysis of the results of numerical climatological and interannual simulations of the marine biogeochemical model (TOPAZ) (i) at a resolution of 0.25 degree forced with CORE fluxes for the period 1949 to 2009 and (ii) at a resolution of 1 degree forced with NCEP fluxes for the period 1978 to 2018 in the global domain are carried out for the study of suboxic zones in the Arabian Sea and Bay of Bengal. The physical model is the modular Ocean Model (MOM5) and the biogeochemical model TOPAZ developed at GFDL has been coupled with MOM5. The model is spun up for 200 years with climatological forcing using bulk formulae to compute surface fluxes.

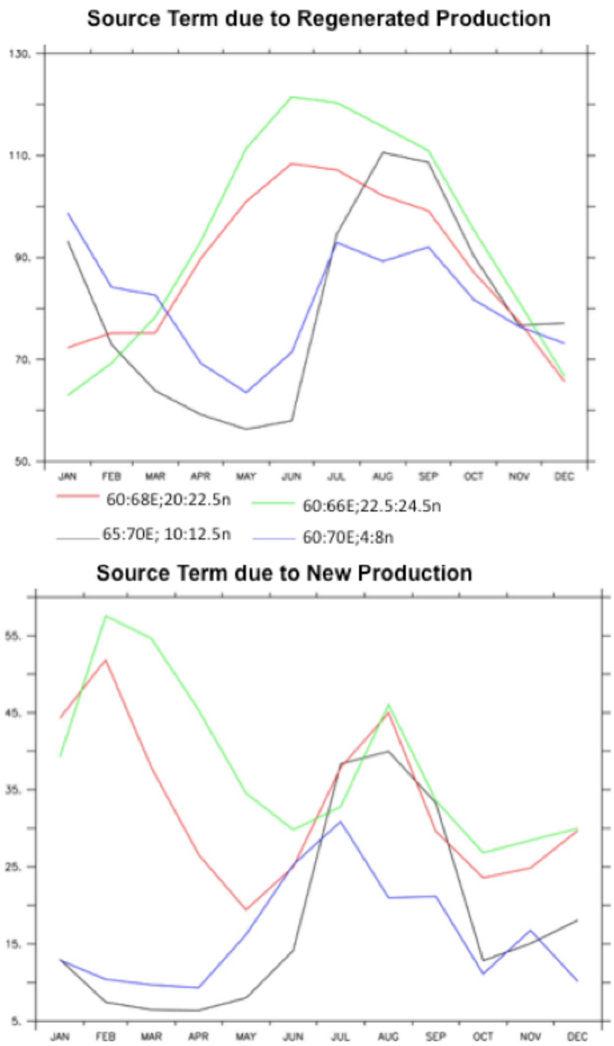

Figure 1.1: Monthly variation of contribution of Regenerated and New Production (mMol/m^2/d) to Oxygen Source Term in the regions of OMZ (60:68^{0}E, 20:22.5^{0}N; 60:66^{0}E, 22.5:24.5^{0}N) and non-OMZ (65:70^{0}E, 10:12.5^{0}N; 60:70^{0}E, 4:8^{0}N) in the Arabian Sea.

Detailed analysis of the source and sink terms of the oxygen equation in the model (TOPAZ) is carried out to understand the contribution of various biogeochemical processes to spatial, seasonal and interannual variations of oxygen concentration in the Arabian Sea (AS) and the Bay of Bengal (BOB). Productivity of large and small phytoplankton, and diazotrophs, due to nitrate (NO3) and Ammonium (NH4) and nitrogen fixation by diazotrophs contribute to the source of oxygen, whereas oxygen is consumed by ammonium produced from non-sinking particles, sinking particles and dissolved organic matter, and for nitrification.

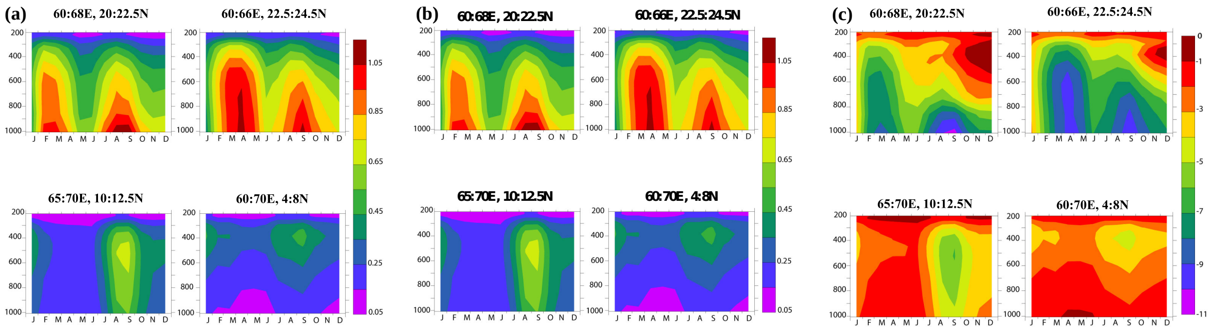

Figure 1.2: Monthly variation of consumption of oxygen with respect to depth in the regions of OMZ and non-OMZ regions (as in Figure 1.1) in the Arabian Sea, due to (a) Remineralization of Detritus (mMol/m^3/d) and (b) Nitrification (mMol/m^3/d), (c) Source minus Sink terms of oxygen (mMol/m^3/d) with respect to depth.

Contribution of total productivity due to NO_3 (New Production) and NH_4 (Regenerated Production) to oxygen source term (Figure 1.1) is higher in the regions of Oxygen Minimum Zone (OMZ) compared to regions in non-OMZs, during all seasons. It can be observed that production of oxygen due to new production is negligible during January-May and October-December in the non-OMZ, whereas it is high during NEM and SWM in the OMZ. Contribution of regenerated production to oxygen source term is high during May-September in the OMZ compared to non-OMZ, and it is higher compared to contribution due to new production during all seasons. It is also noted that both new and regenerated production are higher in the regions of OMZ compared to non-OMZ regions during many months, and regenerated production is higher than new production during all seasons. Variations of sink terms of oxygen with respect to depth for four regions two each in OMZ (60:68^{0}E, 20:22.5^{0}N; 60:66^{0}E, 22.5:24.5^{0}N) and non-OMZ (65:70^{0}E, 10:12.5^{0}N; 60:70^{0}E, 4:8^{0}N) in the AS are analysed in detail. It is noted that the consumption of oxygen due to production of NH_4 from grazing, heterotrophs and dissolved organic nitrogen (LDON and SDON) is negligible (figure not shown), whereas consumption of oxygen for nitrification and remineralization of detritus are very high in the regions of OMZ between 200 and 1000m depth. Consumption for (i) Remineralization of detritus is maximum during February-May and August-October (Figure 1.2a) and (ii) Nitrification is very high during March-December (Figure 1.2b).

Variation of Source minus Sink terms (JO_2) with respect to depth for four regions in the AS is shown in Figure 1.2c. It is observed that JO_2 is negative and higher in magnitude during all seasons in the regions of OMZ compared to the regions in non-OMZ, between 200 and 100m depth. Since JO_2 is negative and having higher values in the OMZ regions, oxygen concentration is very low between 200 and 1000m depth (Figure 1.3). It can be summarized that consumption of oxygen due to remineralization and nitrification processes at depths below 200m are responsible for the low oxygen concentration between 200 and 1000m depth in the OMZ.

Variation of source and sink terms of Oxygen are analysed for one of the regions (89:90^{0}E, 14:15^{0}N)in the OMZ of Bay of Bengal. The term representing the Source minus Sink (JO_2) is negative between 200 and 1000m depth and is high in magnitude during January to April, leading to very low concentration of Oxygen (< 10 m Mol/m3) between 200 and 600 m depth during all seasons. It is noted that consumption of oxygen due to remineralization and nitrification processes at depths below 200m are very high as in the Arabian Sea (figure not shown).

Interannual variation of carbon flux at the air-sea interface and pCO_2 from model simulations,

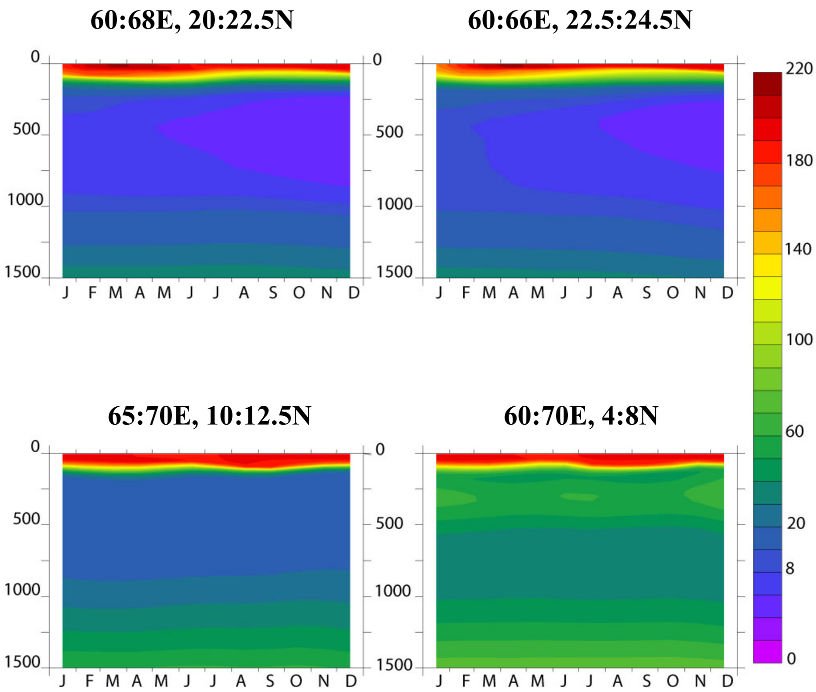

Figure 1.3: Monthly variation of Oxygen (mMol/m^3) with respect to depth in the regions of OMZ and non-OMZ (as in Figure 1.1) in the Arabian Sea.

for two regions in the OMZ and one region in the non-OMZ during 2006 to 2008 is shown in Figure 1.4. It can be observed that both carbon flux from ocean to atmosphere and pCO_2 are higher for the regions in OMZ compared to a region in non-OMZ. Detailed analysis of physical, chemical and biological processes like upwelling, primary productivity, recycling of nutrients etc. will be carried out to understand the carbon and nitrogen cycle in the OMZ regions of north Indian Ocean. Comparison of spatial and seasonal variations of various biogeochemical variables and fluxes from CORE and NCEP simulations in the north Indian Ocean are being carried out.

1.2 Greenhouse gases data collection and analysis

Measurements of greenhouse gases continued through the year at the stations Hanle, Pondicherry and Hoskote, setup by CSIR-4PI, as per WMO standard. Also, discrete sampling of air through flask measurements are done at these stations. The stations were regularly maintained and continuous data from these stations were collected at regular intervals. The data collected from these GHG stations are processed with ICOS protocol and are plotted to see year to year variations. The database of greenhouse gases generated can be used to identify sources and sinks of anthropogenic carbon using advanced inverse modelling techniques.

1.2.1 Measurements at Hanle

The within-hour standard deviation of CO_2 for 2020 is shown in Figure 1.5(a). It can be seen that of the 8637 hourly values, nearly 70% have a standard deviation less than 0.1 ppm, indicating that there is very little within-hour variability at the site. Besides variability at noon (UTC) and midnight (UTC) are also very similar. As Hanle is in an elevated cold desert with very little diurnal variability and minimal local influence, all 24-hour data can be considered for processing.

The daily means of carbon dioxide along with a curve consisting of a constant, linear, quadratic

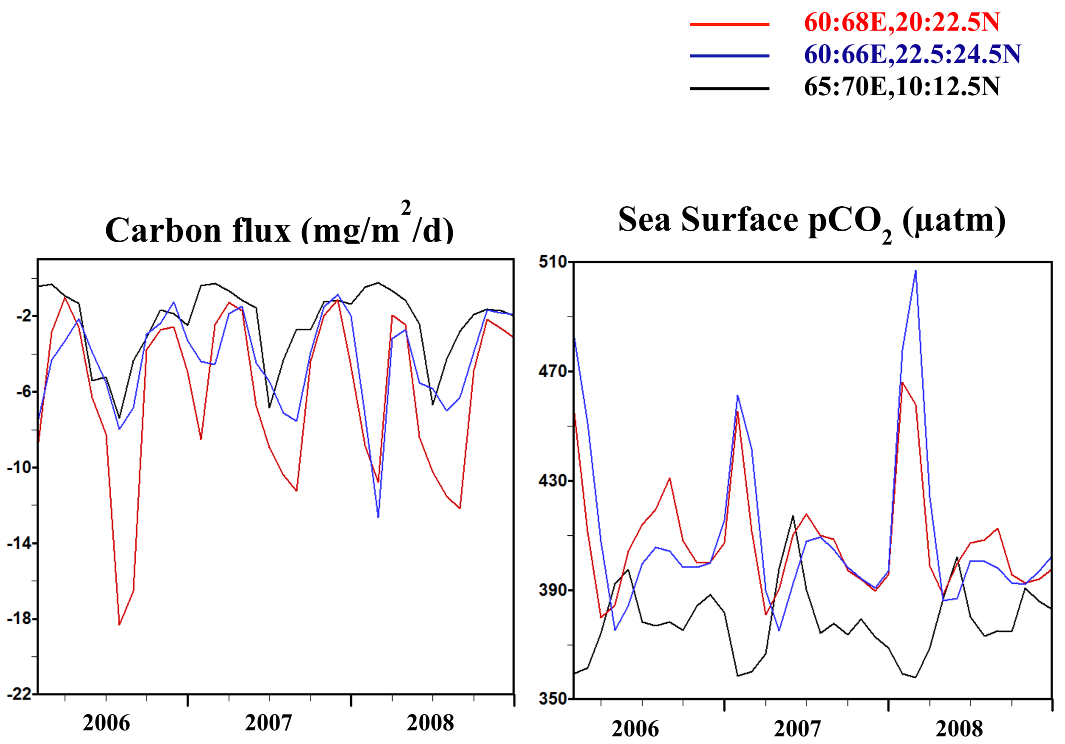

Figure 1.4: Interannual variation of Carbon Flux at the surface of the ocean (mg C/m^2/d) and pCO_2 (μatm) in two regions of OMZ and one region in the non-OMZ from two model simulations (forced with CORE fluxes at 1 degree resolution) for the years 2006-2009.

and 4 harmonics terms at Hanle is shown in Figure 1.5(b). The change in the annual average between 2019 and 2020 is roughly 2.5 ppm indicating a global atmospheric loading of 5.3 Giga tonnes of carbon.

The daily means and the function fit for CH_4 are given in Figure 1.5(c). In contrast to the minimum in CO_2 during monsoon months, CH_4 is maximum in this period. The air reaching Hanle has picked up CH_4 from paddy cultivation and wetlands as it flows over northern India. The increase in the annually averaged CH_4 from 2019 to 2020 is 15 ppb.

The wind is mostly from SW, SSW direction reaching average speeds of 6-7 m/s as shown in Figure 1.5(d). The CO_2 concentration is lowest when the wind is from these directions and is highest when it is easterly or westerly.

The data from Pondicherry was processed similarly for CO_2 and CH_4 and which show similar year to year variation for CO_2 and CH_4 as seen in Hanle.

1.2.2 Measurements at Hoskote

Four species CO_2, CH_4, CO and N_2O are measured here. Figure 1.6(a) shows the daily data and function fit of CO_2. Unlike Hanle, there is a lot of scatter due to local influence. The increase in annual average CO_2 from 2019 to 2020 is 2.3 ppm. Methane measurements can be seen in Figure 1.6(b). There is an increasing trend with an annual increase of 20 ppb between 2019 and 2020.

Carbon monoxide measurements seen in Figure 1.6(c) do not show the trend seen for CO_2 and CH_4. There is a pronounced annual cycle with double peaks in January and April and a minima in August. The amplitude is over 100 ppb. Nitrous oxide increased from 331 ppb to 335 ppb over three years indicating an increase in industrial activity around Hoskote as can be seen in Figure 1.6(d).

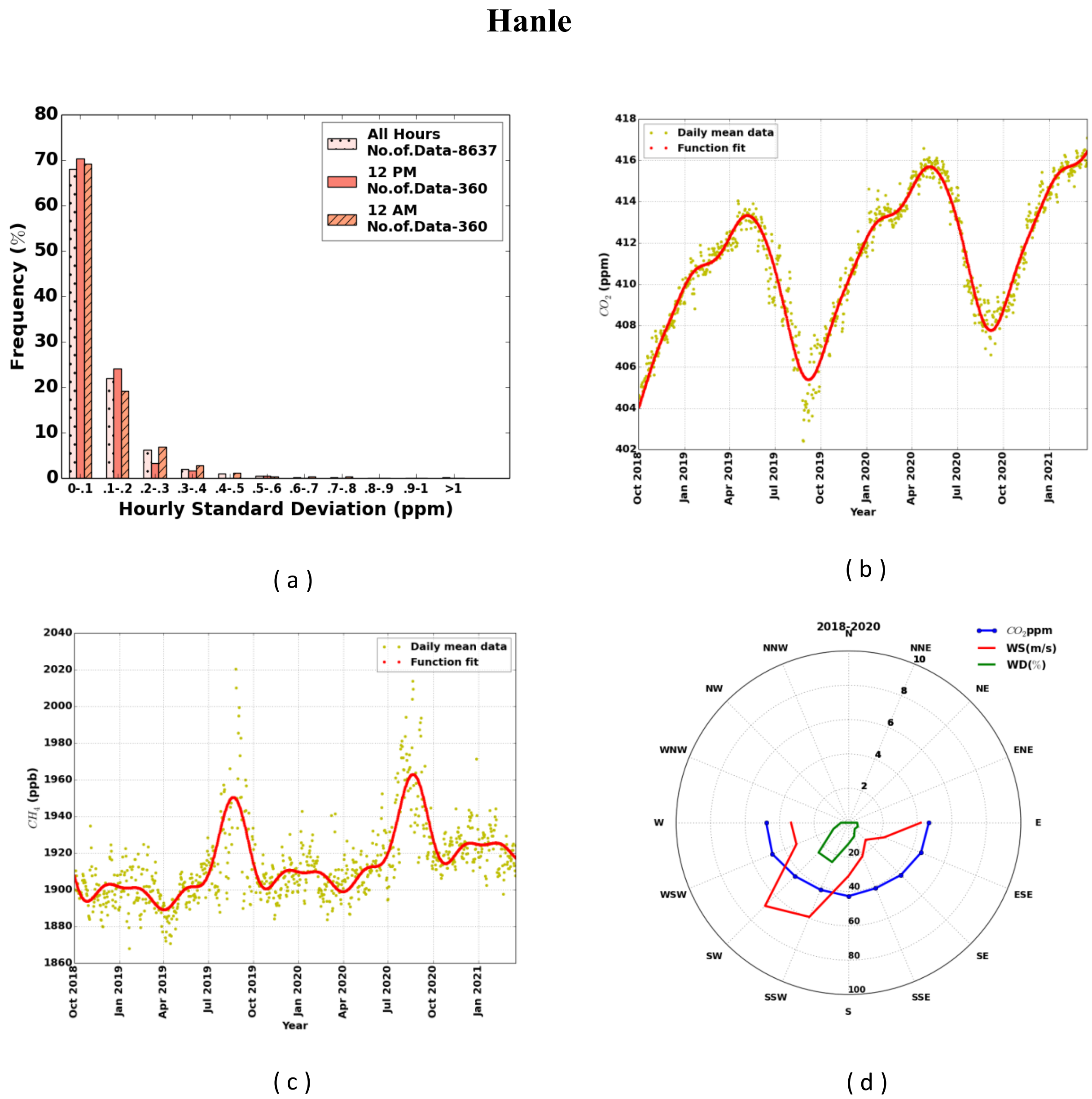

Figure 1.5: Frequency table of hourly standard deviation in 2020 at Hanle (b) Daily-mean data and function fit for CO_2 (ppm) (c) Daily mean data and function fit for CH_4 (ppb) (d) Rose plot of CO_2 (ppm) (measured value – 406 ppm), wind speed (m/s) and wind direction frequency percentage. The scales for CO_2 (ppm) and wind speed (m/s) go from 0 to 10 while wind frequency percentage goes from 0 to 100.

1.2.3 Diurnal Variation at Hoskote

The wind speed and wind direction at Hoskote for summer and monsoon seasons are shown in Figure 1.7. Wind in winter is from the east, in summer from SE-SSW and during monsoon from WSW and post monsoon S-SW. Wind speeds are highest in monsoon reaching speeds of 5.3 m/s around 6:00 UTC. The highest values of CO_2 and CH_4 are around 430 ppm and 2.1 ppm, respectively, in summer around midnight UTC. Enhanced vertical mixing and photosynthetic activity lead to reduction in CO_2 during daytime hours. The amplitudes of the diurnal variation for

Hoskote

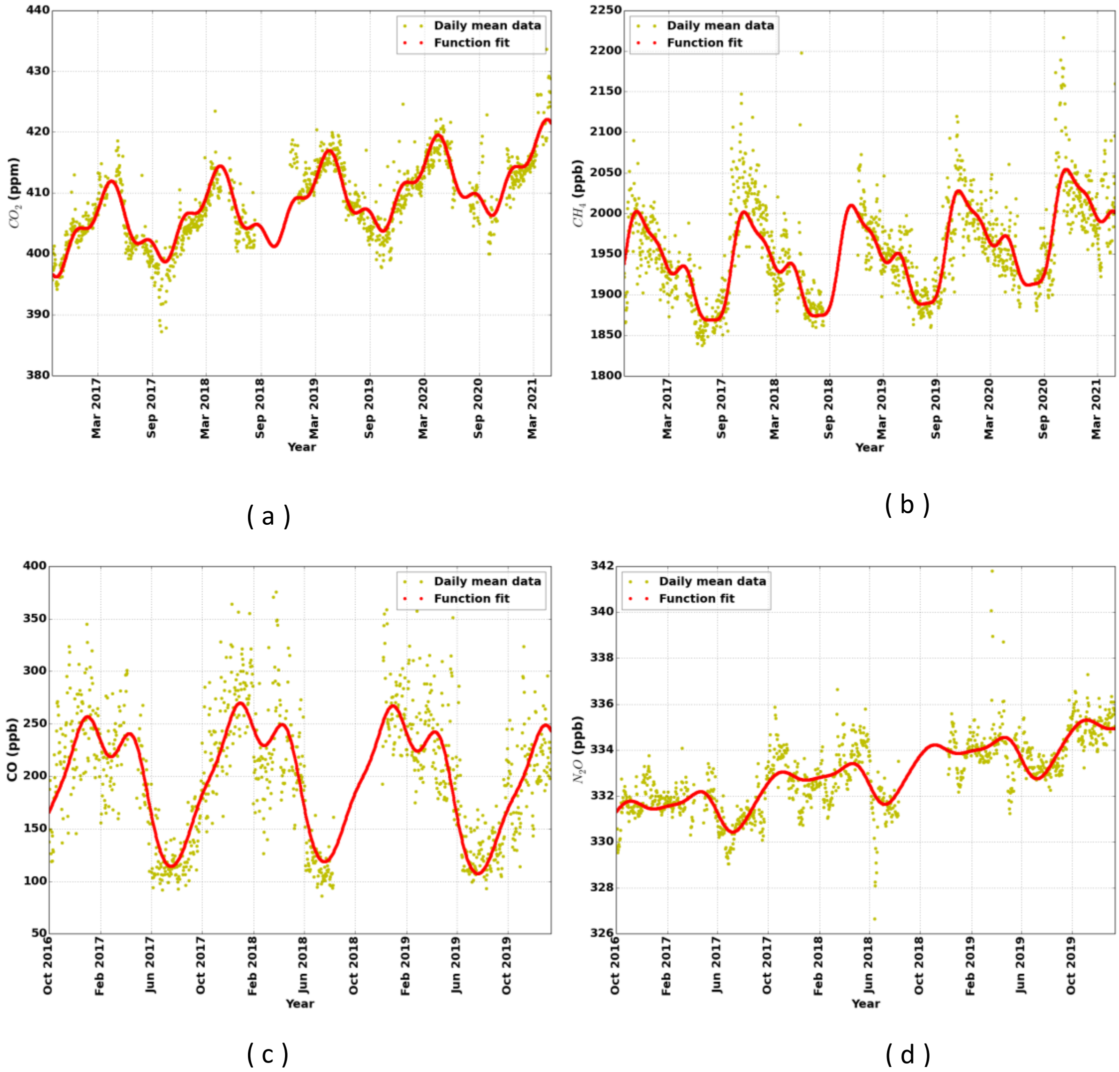

Figure 1.6: Daily mean data and function fit for CO_2 (ppm) (b) Daily mean data and function fit for CH_4 (ppb) (c) Daily mean data and function fit for CO (ppb) (d) Daily mean data and function fit for N_2O (ppb).

CO_2 are around 13, 15, 13 and 22 ppm in winter, summer, monsoon and post monsoon seasons. The amplitudes in case of CH_4 range from 0.08 to 0.17 ppm approximately.

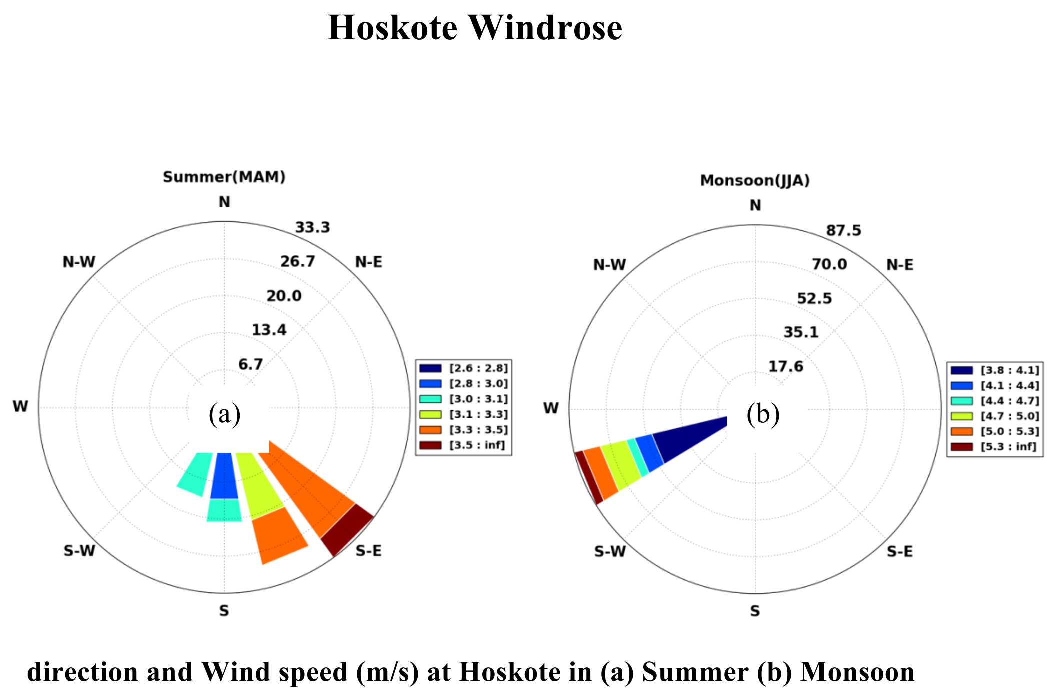

Figure 1.7: Rose plot of wind direction and Wind speed at Hoskote in (a) Summer (b) Monsoon.